Proceedings of the IASS 2024 Symposium
Redefining the Art of Structural Design
August 26-30, 2024, Zurich Switzerland
Philippe Block, Giulia Boller, Catherine DeWolf,
Jacqueline Pauli, Walter Kaufmann (eds.)

Experimental study on wind uplift resistance of metal roofing system for large-span structures

Tianxiong ZHANG[a,*], Yuanqing WANG[a], Jingfeng WANG[b], Wan YI[c], Tingyi LI[c], Qunshan ZHANG[c]

*Department of Civil Engineering, Tsinghua University
No.30, Shuangqing Road, Haidian District, Beijing 100084, China
txzhang@mail.tsinghua.edu.cn

[a] Department of Civil Engineering, Tsinghua University
[b] College of Civil Engineering, Hefei University of Technology
[c] Beijing Urban Construction Group Co., Ltd.

Abstract

Metal roofing systems are widely employed in large-span spatial structures. Characterized by their lightweight and complex connection structures, these roofing systems are prone to structural vulnerabilities, particularly in the presence of strong winds, leading to potential wind uplift damage. To investigate the wind uplift resistance performance of such roofing systems, this study focuses on the metal roofing system of Hefei Xinqiao International Airport Terminal 2. Two full-scale roof specimens, derived respectively from the roof panel and decorative panel components of the metal roofing system, were subjected to static wind uplift tests. The variations in displacement and strain of roof specimens during the loading process were measured. An examination was conducted on the deformation condition of the roofing system due to damage, along with its failure modes, revealing the underlying mechanisms and principles governing its structural breakdown. The research results indicate that the static wind uplift resistance limits for the roofing panel specimen and the decorative panel specimen are 13.3 kPa and 4.9 kPa, respectively. During the failure of the roofing panel specimen, detachment occurs between the support and the standing seam panel, resulting in a bulge in the roofing panel. In the case of the decorative panel specimen, during failure, the support undergoes straightening, leading to detachment from the standing seam panel. The research results provide a scientific basis for the application of these roofing systems in large-span structures.

Keywords: metal roofing system, wind uplift resistance, experimental study, failure mode.

1. Introduction

Metal roofing refers to a type of roofing that employs metal panels as the material, combining the structural and waterproof layers into a single cohesive form. Compared to foreign developments, the metal roofing system industry in China started relatively later, with initial choices of metal roofing materials and structural forms being limited [1]. However, since the early 21st century, driven by rapid urban development and continuous advancements in new materials and technologies, metal roofing systems have evolved from initially using self-tapping screws to perforate roof panels directly, to diverse structural forms such as overlapping, crimping, interlocking, and continuous welding [2,3].

The standing seam metal roofing system, a typical representative of metal roofing, is characterized by its lightweight, durability, excellent waterproofing, and ease of installation. It has been extensively applied in large-span structures such as airport terminals and sports stadiums [4,5]. However, the inherent lightweight and mechanical interlock connections of the standing seam metal roofs have led to

relatively poor wind uplift resistance, resulting in frequent incidents of wind damage in recent years [6]. Instances such as the damage to the roof of Wuhan Tianhe Airport's Terminal 2 by a brief severe wind, the repeated uplift of Quanzhou Train Station's roof by Typhoon Meranti, and three instances of wind uplift damage at Beijing's Terminal 3 have significantly hindered the application and development of standing seam metal roofing systems in China.

Currently, scholars have conducted research on the wind uplift resistance of standing seam metal roofing systems. Habte [7] conducted extensive full-scale roof wind uplift tests and found that the failure was due to weak spots at the seam interlocks. Dong [8] conducted experimental research on the positive and negative load-bearing capacities of aluminum roofing, discovering that the failures were caused by the disconnection between aluminum supports and the panel surface, and that the bearing capacity under negative loading was only 25% of that under positive loading. Damatty [9] established a three-dimensional finite element model of the standing seam metal roof using equivalent springs and analyzed the stress characteristics under wind uplift loads, finding that equivalent springs effectively simulate the mechanical behavior of the seams. Ali [10] studied the dynamic characteristics of roofing under dynamic loads through finite element simulation, noting significant effects of purlin stiffness and the use of anti-wind clips on the dynamic characteristics of the roof. Chen [11] conducted multi-parameter finite element simulations of the wind uplift resistance of standing seam metal roofs based on the concept of equivalent springs, elucidating the impact of various parameters on wind uplift resistance. Shi [12] replaced T-shaped supports with equivalent springs to simulate their support in the horizontal direction and confirmed through finite element simulation that the positive load failure of the standing seam metal roof was the result of combined bending and shearing forces on the supports.

This paper takes the metal roofing project of the Hefei Xinqiao International Airport Terminal 2 as a background, selecting two typical metal roofing specimens to conduct static wind uplift tests. The displacements and strains at key positions were measured, the mechanical properties and deformation characteristics of the roofing system were investigated, and the failure mechanisms were revealed, providing data support and reference for the design and construction of related engineering projects.

2. Project overview

The experimental research object is the metal roofing system of the Hefei Xinqiao International Airport Terminal 2, primarily using standing seam roof panels and aluminum honeycomb decorative panels, as detailed in Figure 1. The structure of the metal roofing system is layered from top to bottom as follows: ①Decorative layer: 25 mm thick aluminum honeycomb panel, ②Partition keel: 50*50*3 mm aluminum alloy square tube, ③Roof waterproof layer: 0.8 mm thick aluminum-zinc coated standing seam steel panel, ④Upper secondary purlins: 150*100*4 mm rectangular steel tube, ⑤Upper main purlins: 200*100*5 mm rectangular steel tube, ⑥Waterproof layer: 1.5 mm thick TPO waterproofing membrane, ⑦Insulation layer: 190 mm thick rock wool panel, ⑧Vapor barrier: 0.3 mm thick PE vapor barrier film, ⑨Support layer: 1 mm thick galvanized profiled steel sheet, ⑩Lower purlins: 200*100*4 mm rectangular steel tube.

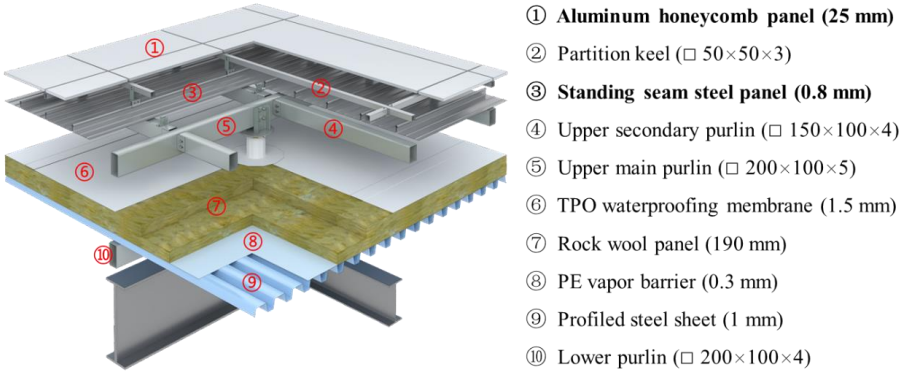

Figure 1: Standing seam metal roofing system

The standing seam roof panels have a width of 405 mm, a thickness of 0.8 mm, and a rib height of 65 mm. These panels are supported on fixed supports and are connected to the purlins using a standing seam point support connection method. The aluminum honeycomb decorative panels measure 3000*1500 mm with a thickness of 25 mm and are secured to the ribs of the roof panels through anti-wind clips and partition keels.

The wind tunnel test report for the Hefei Xinqiao International Airport Terminal 2 [13] indicates that the maximum negative wind pressures for the eave area (standing seam roof panels) and the main area (aluminum honeycomb decorative panels) are 2.91 kPa and 1.35 kPa respectively for a 50-year recurrence period. When converted to a 100-year recurrence period, these values are respectively 3.33 kPa and 1.54 kPa. For static tests, the wind uplift resistance should be twice the standard wind load value, hence the static wind uplift pressures should at least reach 6.66 kPa and 3.08 kPa respectively.

3. Test programme

3.1. Specimen design

According to the actual engineering project, two full-scale metal roofing specimens were designed and fabricated, with details provided in Table 1. Specimen W1 is a standing seam roof panel specimen, composed of layers ③④ as shown in Figure 1. Specimen W2 is an aluminum honeycomb decorative panel specimen, consisting of layers ①②③④ as depicted in Figure 1. The main material properties of each layer of the specimens are shown in Table 2. To verify the applicability of the standing seam metal roofing system in the metal roofing project of Hefei Xinqiao International Airport Terminal 2, the roofing system components used in the test and the construction machinery are consistent with the actual practices at the project site. The layout of the specimens is shown in Figures 2 and 3.

Table 1: Summary of specimen information

Specimen	Purlin spacing (mm)	Number of fixed supports	Number of anti-wind clips	Layer
W1	600	117	—	③④
W2	1200	63	42	①②③④

Table 2: Main material properties of specimens

Structural layer	Material	Yield Strength (MPa)	Elastic Modulus (GPa)
Aluminum honeycomb panel	3003-H24	145	70
Partition keel	6061-T6	245	70
Standing seam steel panel	S300GD	300	206
Purlin	Q355B	355	206
Fixed support	Q355B	355	206
Anti-wind clip	6063-T6	160	70

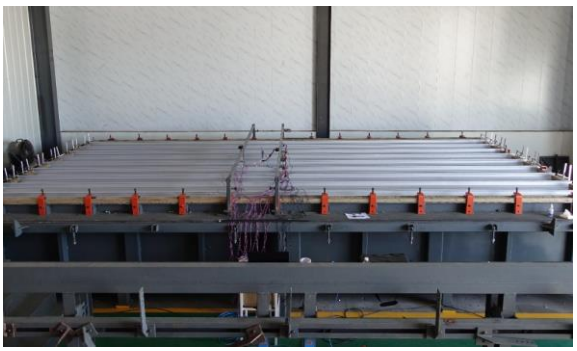

(a) Photo

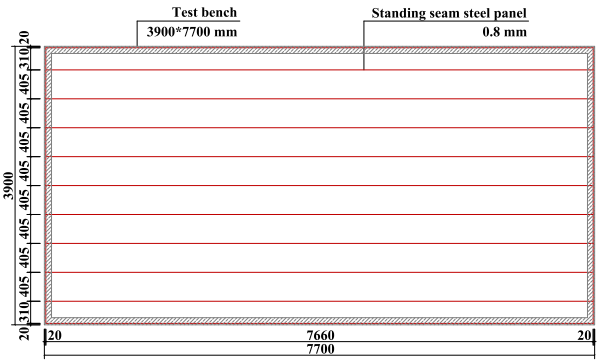

(b) Plan view

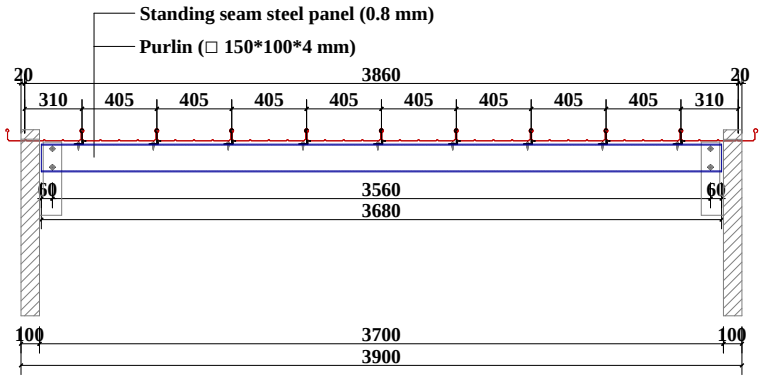

(c) Cross-section view

Figure 2: Specimen W1 arrangement

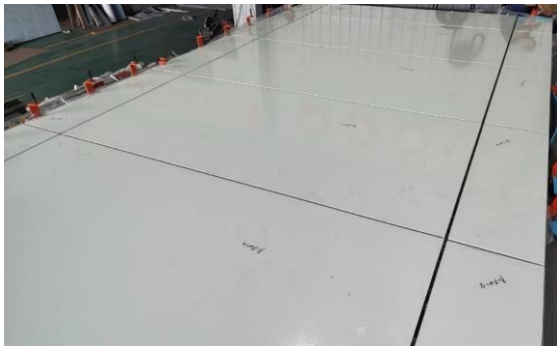

(a) Photo

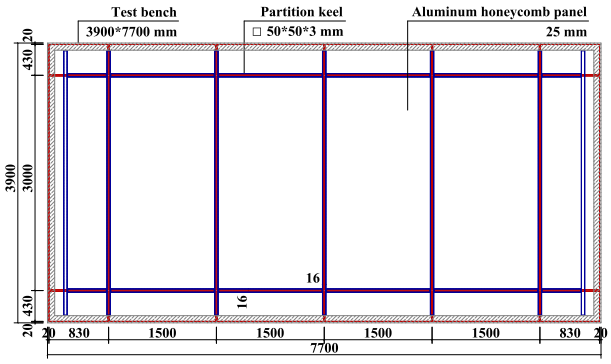

(b) Plan view

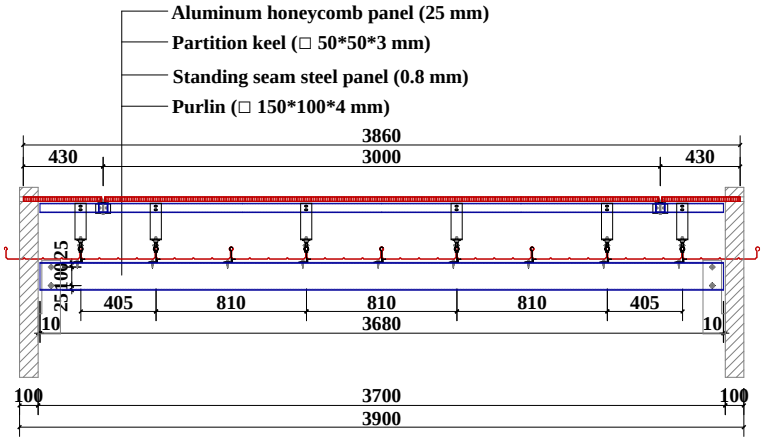

(c) Cross-section view

Figure 3: Specimen W2 arrangement

As shown in Figure 4, the fixed support is a crimping type support, which consists of an upper vertical part and a base. The upper bent arc of the vertical component is connected to the roofing panels on both sides using a clipping and pressing connection. The base is secured to the purlins with self-tapping screws. When subjected to wind uplift loads, the bent arc of the support cannot directly pull out. Instead, it will slide and gradually straighten under the combined action of the squeezing force and pulling force exerted by the locking metal panels on both sides, until it detaches.

As shown in Figure 5, the anti-wind clip consists of two parts: a male buckle and a female buckle. The bottom end is shaped into an arc, and the inner side is made into a toothed design. The male buckle and the female buckle are clamped onto the ribs of the standing seam roof panels and fastened with bolts.

The partition keel of the decorative panel is connected to the upper surface of the anti-wind clip, thus securing it to the anti-wind clip.

(a) Photo

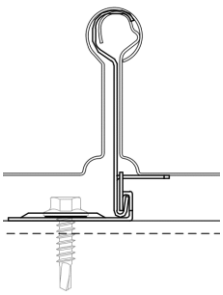

(b) Detail

Figure 4: Fixed support

(a) Photo

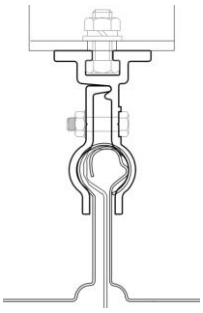

(b) Detail

Figure 5: Anti-wind clip

3.2. Test setup

The experiment was conducted in the enclosure system laboratory of Shanghai Xinxinjie Quality Inspection Co., Ltd., using a roofing comprehensive performance testing machine that is certified by FM Approvals. The dimensions of the test bench are 7700*3900 mm, and the test setup is shown in Figure 6. When installing specimen W1, first secure the purlins to the test bench and fix the supports on the purlins. Then, lay the roof panels from one side to the other in sequence, connecting adjacent roofing panels via a seaming machine. When installing specimen W2, based on the setup of W1, continue by securing the anti-wind clips to the ribs of the roofing panels, and connect the partition keels to the anti-wind clips, finally securing the decorative panels to the partition keels. It is important to note that both specimens W1 and W2 require a layer of polyethylene film to be laid under the roof and decorative panels to form a sealed space, in order to apply negative wind pressure on the roof and decorative panels.

(a) Photo

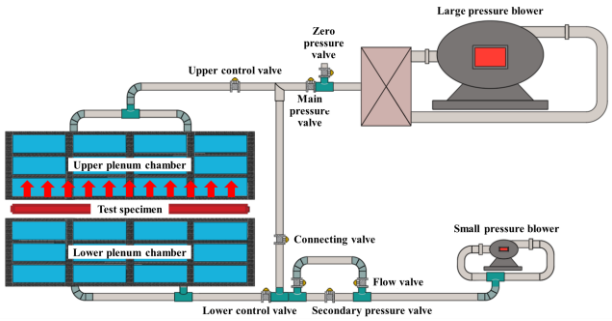

(b) Schematic diagram

Figure 6: Test setup

3.3. Loading regime

The loading regime of an experiment significantly impacts data collection and the results of the test. Therefore, selecting an appropriate loading regime is crucial in the experimental design. For laboratory testing of the wind uplift resistance of standing seam metal roofing systems, the static step-loading method is commonly employed. Accordingly, this experiment is conducted with graded loading in accordance with the Chinese standard GB 50205-2020 [14]. The loading regime schematic is shown in Figure 7, and the main loading process is as follows:

(1) Start from 0, pressurizing at a rate of 0.07 kPa s^{-1} to 0.7 kPa. (2) Load to the specified pressure level and maintain that pressure for 60 seconds, then release the air to return to 0. (3) Repeat the above steps, increasing by 0.7 kPa for each level as the next pressure level, each pressure level should be maintained

for 60 seconds, then release the air to return to 0. (4) Continue the loading process until the specimen fails or breaks, stop the test and record the pressure value of the level before failure.

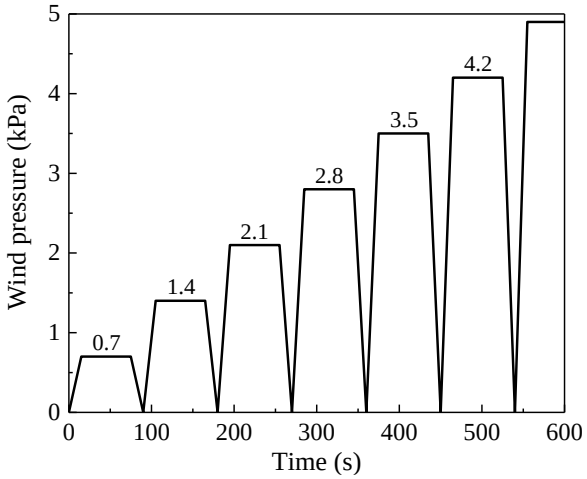

Figure 7: Loading regime

3.4. Measurement scheme

The measurements in this experiment primarily include the displacement and horizontal and vertical strains at different parts of the roof panel's outer surface under stable wind pressure, as well as the ultimate wind pressure at the time of failure. The layout of the LVDTs and strain gauges is shown in Figure 8. Due to the significant instantaneous deformation that occurs when the specimen fails, in order to ensure the safety of the testing equipment, the LVDTs are removed once the deformation reaches a certain level, hence the LVDTs could not record the complete displacement curve. Additionally, due to experimental constraints, the displacement and strain of specimen W2 were not measured.

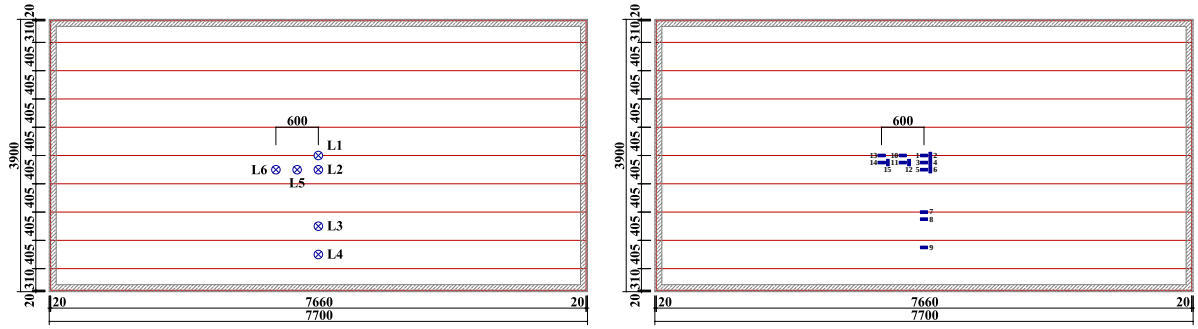

(a) LVDTs layout (b) Strain gauges layout

Figure 8: Measurement system layout diagram

4. Test results

4.1. Failure Mode

4.1.1. Specimen W1

The experiment was divided into two loading stages, demarcated by the moment when the LVDTs were removed. In the first loading stage, as the load increases, the roof panel exhibited varying degrees of bulging. The displacement from the bulging increased with the applied load, with significant bulging occurring at the mid-span of the panel. When the load reached 10.5 kPa, the LVDTs were removed. At

this point, a slight opening at the seams was observed, and minor support marks were found on the vertical ribs of the lower roof panel at the contact points with the supports, as shown in Figure 9.

In the second loading stage, a loud noise occurred when the load was increased to 14.0 kPa, indicating severe disengagement at the seam engagement areas of the standing seam steel panel at the mid-span, as shown in Figure 10. No significant straightening of the upper bent arcs of most supports was observed, and the ultimate wind pressure was determined to be 13.3 kPa.

(a) Seam opening (b) Support mark

Figure 9: Local deformation of roof panel

Figure 10: Roof panel seam disengagement

4.1.2. Specimen W2

As the load gradually increased, the decorative panel exhibited varying degrees of bulging. The bulging displacement increased progressively with the increasing load, with significant bulging observed at the mid-span of the panels. When the load reached 5.19 kPa, a loud noise occurred, indicating substantial straightening of the upper bent arcs of some supports, resulting in their detachment from the roof panel. Additionally, the upper vertical parts of some supports detached from their bases, as shown in Figure 11. Despite these occurrences, both the roof panels and the anti-wind clips remained undamaged. The ultimate wind pressure was determined to be 4.9 kPa.

(a) Support straightening (b) Support pull-out

Figure 11: Support failure

4.2. Ultimate wind pressure

Ultimate wind pressure is a critical parameter for assessing the wind uplift resistance of standing seam metal roofing systems. The ultimate wind pressures recorded at the time of failure for the two specimens are listed in Table 3. According to the Chinese standard GB 50205-2020 [14], the wind uplift coefficient, K, should exceed 2.0, as shown in Equation (1). As indicated in Table 3, the ultimate wind pressure values for both specimens meet the regulatory requirements.

$$K = \omega_u / \omega_s \geq 2.0 \quad (1)$$

where K is the wind uplift coefficient, ω_u is the wind uplift pressure value, that is, the ultimate wind pressure, and ω_s is the standard value of wind load.

Table 3: Test results

Specimen	ω_u (kPa)	ω_s (kPa)	K
W1	13.3	3.33	3.99
W2	4.9	1.54	3.18

4.3. Displacement and strain

The load-displacement curves and load-strain curves for specimen W1 are shown in Figures 12 and 13, respectively. From Figure 12, it is evident that during loading, the deformation of the roof panel generally shows an approximately linear increase with load, indicating that it is in the elastic deformation stage. The deformation at the mid-span of the roof panel (L2~L6) is significantly greater than the deformation at the rib interlock (L1).

Figure 13 reveals that the roof panel is primarily subjected to lateral forces, with the longitudinal forces being considerably smaller in comparison. The maximum lateral strain occurs at SG6, and the difference between lateral and longitudinal strains is most pronounced here, with the longitudinal strain being approximately 2.3% of the lateral strain. At the top of the seam, SG2 shows virtually no strain under lower loads, which then rapidly increases with the load, indicating that there is almost no relative sliding at the seam under lower loads.

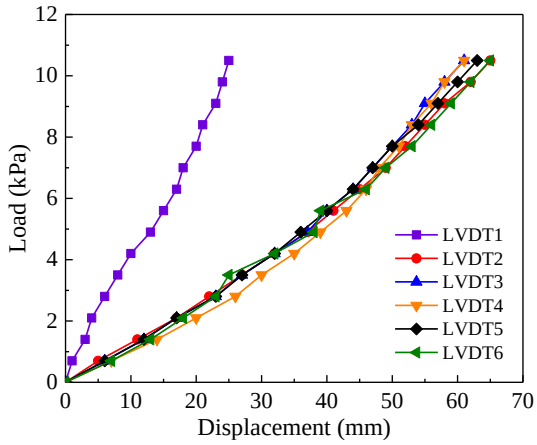

Figure 12: Load-displacement curves

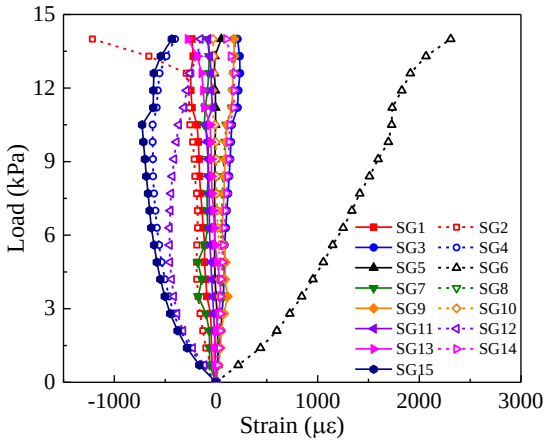

Figure 13: Load-strain curves

5. Conclusion

(1) The static wind uplift resistance values for the standing seam roof panel specimen W1 and the aluminum honeycomb decorative panel specimen W2 are 13.3 kPa and 4.9 kPa, respectively. Both values exceed twice the standard wind load value, meeting the wind uplift design requirements.

(2) Under wind uplift loads, the main failure modes of the standing seam metal roofing system are disengagement at the seam interlock and straightening of the supports. This indicates that the seam

interlock connections are the weak points of the standing seam metal roofing system. Therefore, in actual engineering projects, these weak points should be reinforced to enhance the overall wind uplift resistance of the standing seam metal roofing system.

(3) The standing seam metal roofing system offers numerous advantages, and its technology has become increasingly mature in China. The research on the metal roofing of Hefei Xinqiao International Airport Terminal 2 can provide a reference for similar engineering designs and constructions, promoting the development of metal roofing systems in China.

References

[1] Zhou M, Fan J S, Liu Y F, et al. Non-uniform temperature field and effect on construction of large-span steel structures. *Automation in Construction*, 2020, 119: 103339.

[2] Azzi Z, Habte F, Vutukuru K S, et al. Effects of roof geometric details on aerodynamic performance of standing seam metal roofs. *Engineering Structures*, 2020, 225: 111303.

[3] Seek M W, Avci O, McLaughlin D. Effective standoff in standing seam roof systems. *Journal of Constructional Steel Research*, 2021, 180: 106590.

[4] Xia Y, Kopp G A, Chen S. Failure mechanisms and load paths in a standing seam metal roof under extreme wind loads. *Engineering Structures*, 2023, 296: 116954.

[5] Mobasher M E, Adams B, Mould J, et al. Damage mechanics based analysis of hail impact on metal roofs. *Engineering Fracture Mechanics*, 2022, 272: 108688.

[6] Xuan Y, Xie Z. Research progress on wind loads and wind resistance bearing capacity of large span metal roof structures. *Journal of Building Structures*, 2019, 40(3): 41-49. (in Chinese)

[7] Habte F, Mooneghi M A, Chowdhury A G, et al. Full-scale testing to evaluate the performance of standing seam metal roofs under simulated wind loading. *Engineering Structures*, 2015, 105: 231-248.

[8] Dong Z, Zhang Q, Shi J. Experiment study and design analysis of aluminum-magnesium-manganese alloy roof panel. *Building Structure*, 2008, 38(3): 69-72. (in Chinese)

[9] El Damatty A A, Rahman M, Ragheb O. Component testing and finite element modeling of standing seam roofs. *Thin-Walled Structures*, 2003, 41(11): 1053-1072.

[10] Ali H M, Senseny P E. Models for standing seam roofs. *Journal of Wind Engineering and Industrial Aerodynamics*, 2003, 91(12-15): 1689-1702.

[11] Chen Y. Loading bearing capacity of the standing seam roof system under the wind load. Beijing: Beijing Jiaotong University, 2015. (in Chinese)

[12] Shi J, Zhang Q, Dong Z. Numerical simulation and experimental analysis on aluminium alloy roof panel. *Building Structure*, 2006(S1): 458-460. (in Chinese)

[13] Quan Y. Hefei Xinqiao International Airport Terminal Area Expansion Project (Non-Civil Aviation Specialty) Terminal 2 Wind Tunnel Test Research Report. Shanghai: Tongji University, 2021. (in Chinese)

[14] GB 50205-2020. Standard for acceptance of construction quality of steel structures. Beijing: China Planning Press, 2020. (in Chinese)

[15] GB/T 51422-2021. Technical standard for test, appraisal and strengthening of metal building envelope system. Beijing: China Planning Press, 2021. (in Chinese)